HHS Public Access

Author manuscript

Int J Radiat Oncol Biol Phys. Author manuscript; available in PMC 2021 February 01.

Published in final edited form as:

Int J Radiat Oncol Biol Phys. 2020 February 01; 106(2): 440–448. doi:10.1016/j.ijrobp.2019.10.049.

Design, Implementation, and in Vivo Validation of a Novel Proton FLASH Radiation Therapy System

Eric S. Diffenderfer, PhD, **Ioannis I. Verginadis, PhD**, **Michele M. Kim, PhD**, **Khayrullo Shoniyozov, PhD**, **Anastasia Velalopoulou, PhD**, **Denisa Goia, MS**, **Mary Putt, PhD**, **Sarah Hagan, MS**, **Stephen Avery, PhD**, **Kevin Teo, PhD**, **Wei Zou, PhD**, **Alexander Lin, MD**, **Samuel Swisher-McClure, MD**, **Cameron Koch, PhD**, **Ann R. Kennedy, PhD**, **Andy Minn, MD, PhD**, **Amit Maity, MD, PhD**, **Theresa M. Busch, PhD**, **Lei Dong, PhD**, **Costas Koumenis, PhD**, **James Metz, MD**, **Keith A. Cengel, MD, PhD**

Department of Radiation Oncology, University of Pennsylvania, Philadelphia, Pennsylvania

Summary

Purpose: Recent studies suggest that ultrahigh-dose-rate, “FLASH,” electron radiation therapy (RT) decreases normal tissue damage while maintaining tumor response compared with conventional dose rate RT. Here, we describe a novel RT apparatus that delivers FLASH proton RT (PRT) using double scattered protons with computed tomography guidance and provide the first report of proton FLASH RT-mediated normal tissue radioprotection.

Methods and Materials: Absolute dose was measured at multiple depths in solid water and validated against an absolute integral charge measurement using a Faraday cup. Real-time dose rate was obtained using a NaI detector to measure prompt gamma rays. The effect of FLASH versus standard dose rate PRT on tumors and normal tissues was measured using pancreatic flank tumors (MH641905) derived from the KPC autochthonous PanCa model in syngeneic C57BL/6J mice with analysis of fibrosis and stem cell repopulation in small intestine after abdominal irradiation.

Results: The double scattering and collimation apparatus was dosimetrically validated with dose rates of 78 ± 9 Gy per second and 0.9 ± 0.08 Gy per second for the FLASH and standard PRT. Whole abdominal FLASH PRT at 15 Gy significantly reduced the loss of proliferating cells in intestinal crypts compared with standard PRT. Studies with local intestinal irradiation at 18 Gy revealed a reduction to near baseline levels of intestinal fibrosis for FLASH-PRT compared with standard PRT. Despite this difference, FLASH-PRT did not demonstrate tumor radioprotection in MH641905 pancreatic cancer flank tumors after 12 or 18 Gy irradiation.

Conclusions: We have designed and dosimetrically validated a FLASH-PRT system with accurate control of beam flux on a millisecond time scale and online monitoring of the integral and

Corresponding author: Keith A. Cengel, MD, PhD; Cengel@pennmedicine.upenn.edu.

Disclosures: L.D. reports personal fees from Varian Medical Systems Speakers Bureau and other from Varian Medical Systems (PI of Master Research Agreement between the University of Pennsylvania and Varian Medical Systems), outside the submitted work. A.L. reports personal fees from Ion Beam Applications Speakers 7Bureau, personal fees from Galera Therapeutics Advisor Board, outside the submitted work.

J.M. reports other from Varian Medical Systems Advisory Board, other from Ion Beam Associates Advisory Board, other from Provision Advisory Board, outside the submitted work.

dose delivery time structure. Using this system, we found that FLASH-PRT decreases acute cell loss and late fibrosis after whole-abdomen and focal intestinal RT, whereas tumor growth inhibition is preserved between the 2 modalities.

Introduction

Proton radiation therapy (PRT) can improve spatial dose delivery compared with photons or electrons. Recent studies suggest that FLASH electron RT decreases normal tissue damage while maintaining tumor response compared with conventional dose rate electron RT,[1-4] but these effects are predominately observed in vivo. Initial studies focusing on the possible effects of FLASH RT dose rates for laser-accelerated protons found no dose rate dependent effects using a variety of in vitro cell culture techniques that included monolayer and 3-dimensional or organoid cultures of both cancer and normal cell lines.[5-7] However, a recent study using 4.5 MeV protons at 1000 Gy/s revealed decreased γ-H2AX foci and increased expression of β-galactosidase and TGFβ compared with 0.05 Gy per second.[8] Using electron or photon RT, FLASH dose rate—dependent normal tissue radioprotection has been demonstrated for functional and pathophysiologic outcomes in brain, lung, bowel, and skin.[1,4,9-13] Although normal tissues are protected by FLASH RT, studies of orthotopic lung and ectopic head and neck cancers demonstrated no evidence of FLASH radioprotection.[1,4,14]

In terms of dose rate thresholds, electron RT >60 Gy/s demonstrated complete or nearly complete protection against cognitive decline induced by 10 Gy whole brain irradiation in mice.[10] This dose rate threshold has been substantiated in other murine models with normal tissue protection noted when increasing from conventional dose rates (~1-2 Gy/min) to 37 Gy/s photon RT or 40 Gy/s, 70 to 210 Gy/s electron RT respectively for pulmonary fibrosis and gastrointestinal radiation syndrome.[1,9,11] These results suggest the exciting hypothesis that the unique temporal effects of the FLASH-PRT dose rate could augment PRT-intrinsic spatial advantages. Standard PRT pencil beam scanning dose rates are higher than conventional electron or photon RT dose rates, with localized areas achieving dose rates of 0.5 to 1 Gy/s. The main goal of this research is to understand the biological effects of proton beams. Although we are capable of performing pencil beam scanning in our clinical treatment rooms, it is important to understand the basic dosimetry and biological effects of dose rates in experimental settings. For this reason, we have designed and constructed a novel RT apparatus that can deliver either FLASH (60-100 Gy/s) or standard (0.5-1 Gy/s) dose rates using double scattered protons in a computed tomography (CT)—defined geometry. We use the single pencil beam in our research room to create a double scatter system so that we can provide a relatively uniform and expanded field size without adding another variable with spot scanning speed. Using this system, we provide the first evidence that compared with standard PRT, FLASH PRT elicits reduced levels of both acute and chronic gastrointestinal damage without radioprotection of pancreatic cancer flank tumors in the same mouse model.

Methods and Materials

Proton delivery and beam modulation

IBA Proteus Plus (Louvain-La-Neuve, Belgium) was used to deliver a 230 MeV (range ~32.0 g/cm^2) beam on the fixed angle beam line in the dedicated research room (Fig. 1A). Beam alignment was confirmed using EBT3 film. Similar to clinical treatments, CT-based imaging is performed for initial treatment planning and then for selected irradiations to verify position of the beam. For all irradiations, target alignment was performed with a laser positioning system providing vertical and horizontal lasers aligned with the proton beam center.[15] Custom 3-dimensional printed jigs with anesthesia gas ports were used to allow irradiation of mice on a small animal radiation research platform with cone beam CT capability.[15]

Beam delivery and control

Proton flux was modulated using an arbitrary waveform generator driving the beam current regulation unit (BCREU) (Fig. 1C). Absolute dose was set by configuring waveform generator pulse widths based on the premeasured dose rate or stopping the current pulse to the BCREU with the output of a preset counter connected to an electrometer. The time structure of the beam pulse was recorded to verify the dose rate. Beam current from the cyclotron was varied within clinical operating parameters, 5 to 300 nA, to achieve the desired dose rate at the target. While the cyclotron generates a quasicontinuous beam during the beam on time, defined by the waveform generator pulse, there is an underlying fine structure of approximately 2 ns beam pulses with a frequency around 106 Mhz corresponding to the cyclotron RF.

Dosimetry and real time monitoring

Absolute dose was measured at multiple depths in solid water using a parallel plate Advanced Markus Chamber with a NIST traceable calibration certificate ($N_{D,w}$ = 1.577 Gy/nC) and applying corrections for temperature, pressure, polarity effects, and recombination according to the International Atomic Energy Agency Code of Practice TRS-398,[16] with beam quality correction (k_Q = 1.001) from Table 31 for the Markus chamber. An online transmission parallel plate chamber was cross calibrated with the absolute dose measurements, and both sets of readings were validated against an absolute integral charge measurement using a Faraday cup.[17] Depth dose profiles were measured with the Markus chamber at multiple depths (FLASH dose rate) and with a multilayer ionization chamber, Zebra (standard dose rate). Beam width, flatness, and symmetry were evaluated at the target position using EBT3 film scanned in an Epson 1000XL flatbed scanner. Irradiated film was analyzed using ImageJ and Matlab software. Prompt gamma rays emitted from nuclear excitations at the beam line exit window were measured using a gamma detector comprised of a NaI(TI) crystal coupled to a photomultiplier tube biased at 900 V. The gamma ray pulse signal from the NaI detector was shaped and amplified with a NIM module and recorded by a 1 GHz oscilloscope. The time-dependent frequency of detected gamma rays was related to the dose rate delivered for each mouse irradiation by dividing the counts into 10 equal time bins and comparing the frequency to dose rate calibration conditions before irradiation using a custom Matlab script.

Murine studies

All animal studies were reviewed and approved by the Institutional Animal Care and Use Committee. Mice were checked daily and euthanized upon onset of severe morbidity including hunched posture, social withdrawal, relative immobility, or apparent weight loss >20%, and isoflurane in medical air was used to anesthetize mice for procedures, including PRT. For the acute radiation damage studies, 8- to 10-week-old C57BL/6J mice (Jackson Labs, Bar Harbor, ME) were randomly assigned to 15 Gy whole abdominal FLASH PRT (78 ± 9 Gy/s) versus standard PRT (0.9 ± 0.08 Gy/s) and intestinal segments were harvested at 3.5 days post-IR and preserved in optimal cutting temperature medium. Flank tumors were generated by injecting with 5 x 10^5 MH641905 cells derived from the KPC autochthonous PanCa model subcutaneously in 8- to 10-week-old C57BL/6J mice. Ten days later (median tumor volume 61 mm^3) mice were randomly assigned to receive 12 or 18 Gy with FLASH or standard PRT to a focal area that encompassed the tumor and the upper intestine. Tumors were measured with calipers 3 to 4 times per week, and when the tumor volume reached around 400 mm^3, randomly selected mice underwent surgical tumor resection to allow assessment of intestinal fibrosis in tumor bearing mice. Irradiated intestinal segments were collected and fixed in 10% formalin 8 weeks post-PRT.

Histology

Intestinal segments were harvested at the site of irradiated area for histologic evaluation. Tissues for Masson's trichrome staining were fixed in 10% neutral buffered formalin for 24 hours before dehydration and paraffin embedding. Coded stained slides were evaluated by an independent researcher. Microscopy was performed on the Nikon Eclipse TE2000-U (Nikon, Melville, NY, USA).

EdU assay

Twenty milligrams per kilogram 5-ethynyl-20-deoxyuridine (EdU) were injected intraperitoneally 2 to 3 hours before euthanasia staining was detected as described previously.[18] EdU + cells/crypt were assessed by counting at least 100 crypts per mouse sections. EdU staining was also used to quantify the regenerated crypts, where a regenerated crypt contains 5 or more EdU + cells with a lumen. EdU staining data were derived from 2 biologically independent experiments. Microscopy was performed on the Zeiss Observer.Z1 (Zeiss, German).

Statistical analysis

For analysis of tumor regrowth, we used an endpoint of 4 times the starting tumor volume. Because some animals in the 18 Gy group experienced more than 20% weight loss, they were euthanized before reaching this regrowth endpoint. Therefore, we fit a proportional subdistribution hazards regression to the data with tumor regrowth as the failure event of interest to compare the cumulative incidence of tumor regrowth between groups. For analysis of fibrosis and crypt cell repopulation, we first summarized the data by animal using simple means. We then compared groups using one-way analysis of variation for the fibrosis and 2-sided Welch T-tests for crypt cell repopulation and, to maintain a family-wise

type I error rate of 0.05, we adjusted for 3 multiple comparisons for each group of comparisons using a Holm-Bonferroni correction.

Results

The depth dose profiles of the FLASH and standard beams demonstrate that the entrance region has comparable and relatively homogeneous dosimetry for target depths within a range of 0 to 15 g/cm^2 (Fig. 1B). We tested 2 operational modes to control the total dose delivered: 1 used a fixed pulse width to set a beam-on time determined by prior dose rate measurements versus a variable pulse width to deliver a preset number of monitor units that were determined by an in-line ionization chamber (Fig. 1C). Both methods produced a linear response with correlation coefficients of 0.9997 or 0.9995 for pulse width or monitor units versus dose, respectively (Fig. 1D). To better understand the time structure of the proton flux within these pulses, prompt gamma rays emitted from nuclear excitations were detected and the data processed as described in the Methods and Materials section. These studies demonstrated that there is potential variation of dose rate within each pulse and suggested that it would be best to use the monitor unit mode to stop the beam to reduce the potential for interrun variation in total dose delivered (Fig. 1E). Using this delivery mode, the dose accuracy as represented by the relative mean absolute difference between prescribed dose and dose measured by the secondary ionization chamber was 0.5% for standard versus 1.1% FLASH conditions. Oscilloscope trace leading and trailing edges of the beam-on pulse sent to the BCREU were compared with the gamma count trace to determine an average beam on/off latency of ~150 microseconds with respect to the beam-on pulse.

In validation studies, Markus chamber and a Faraday cup dose measurement yielded the same response curve throughout available beam energies (Fig. 2A). The ratio of charge collected by the Faraday cup, which will not saturate or suffer from recombination effects at these dose rates, and Markus chamber was stable from 0 to 300 nA proton current (Fig. 2B). The Markus chamber demonstrated no evidence of signal loss owing to recombination for bias voltages greater than 200 (Fig. 2B, inset). Separate (FLASH and standard) recombination correction factors were used for absolute dose measurements. The factors were measured at each experiment and calculated using the TRS-398 protocol for pulsed beams. For FLASH dose rate average $k_S = 1.004 \pm 0.005$ and for standard dose rate average $k_S = 1.003 \pm 0.003$. The dose rate achieved in the “entrance” portion of the beam for currents up to 300 nA is linear as measured by a Markus chamber (Fig. 2C), and the primary ionization chamber is also linear with beam current (Fig. 2D). The 3-dimensional uniformity of the collimated beam was measured using EBT3 film in solid water phantoms for the 1 x 2 cm collimator used in animal studies, in which straight lateral beam treats either the whole or upper abdomen of a mouse (depending on the collimator rotation) with 100% of the target covered by 90% to 95% of the desired dose (Fig. 3).

To test the feasibility of this technical approach and obtain preliminary evidence of possible FLASH-PRT efficacy, whole abdominal and focal irradiation of C57BL/6J mice was delivered using standard (0.9 ± 0.08 Gy/s) versus FLASH (78 ± 9 Gy/s) dose rates. In studies of acute intestinal damage after 15 Gy whole abdominal PRT, FLASH-PRT mice showed a significantly higher number of proliferating cells per crypt than standard-PRT

mice as measured by EdU incorporation, although both were significantly decreased compared with the nonirradiated tissues (Fig. 4A, 4B). Additionally, FLASH-PRT preserved a significant higher percentage of regenerated crypts in comparison to the standard PRT (Fig. 4C). To further investigate a potential difference on the impact of the 2 treatment modalities on normal tissue damage, we evaluated the development of intestinal fibrosis as a long-term effect post-PRT. Mice exposed to a focal intestinal irradiation at 18 Gy and intestinal segments harvested at 8 weeks post-IR. Masson's trichrome staining revealed a pronounced fibrosis development on the standard irradiated intestines, which is significantly reduced in the group of Flash irradiated intestines ($P = .0014$), with the latter qualitatively resembling nonirradiated tissues (Fig. 4D, 4E).

Finally, to evaluate the effect of both treatment modalities on tumor growth, we used a pancreatic flank tumor model. Both treatment modalities presented a similar dose-dependent inhibition on tumor growth after 12 and 18 Gy (Fig. 5A, 5B). Cumulative incidence of tumor regrowth to 4 times the starting tumor volume was decreased by PRT ($P < .000001$), but not different between FLASH and standard PRT (12 Gy $P = .68$; 18 Gy $P = .84$).

Discussion

Because the FLASH effect has been observed for dose delivered in time scales on an order of magnitude around 100 ms, it is likely that the underlying biological mechanism will be influenced on a similar time scale, and a clear picture of the delivery time structure is, therefore, critical for future biological studies and comparison of radiation delivery technologies. Moreover, precise dosimetry and dose administration is a critically important problem when studying FLASH biology so that the experimentalist can be confident that any observed biological differences arise solely from dose rate and not total dose delivered. Unlike previously described FLASH-PRT designs,[19] the apparatus described in this manuscript uses proton beam current as the determinant of dose rate and all other elements from the cyclotron, through the beamline, scatters, monitors, and sample or animal restraint jig, are completely identical. By design, this means that the only possible difference between FLASH and standard conditions for this setup is dose rate. Moreover, the ability to verify the time-dose structure within each pulse using a gamma counter provides real-time feedback during an experiment for beamline optimization and allows post hoc analysis of the potential biological implications of the actual dose rate and time structure that was delivered to each animal. Along with real-time monitoring of the integral dose delivery and time structure, the ability to validate the performance of our dosimetry devices at FLASH dose rates with multiple methods provides increases confidence in the precision and accuracy of beam delivery and reduces dosimetric uncertainty that might confound the interpretation of biological outcomes.

The success of radiation therapy depends on the ability to target and eliminate malignant cells with radiation while simultaneously limiting damage to surrounding normal tissues. Using a mouse model of combined syngeneic heterotopic pancreatic tumors and upper intestinal track injury, we show that FLASH PRT elicits significantly reduced intestinal fibrosis compared with standard PRT. Notably, this tissue-sparing effect of FLASH PRT did not extend to tumor response in the same animals, which essentially translates to an

increased therapeutic window for this modality. Moreover, FLASH PRT appeared to result in a more transient inhibition of proliferating crypt cells compared with standard PRT 3.5 days after treatment. Interestingly, analysis of the proliferation at 1 day post-PRT did not demonstrate any significant difference between the 2 modalities (not shown), suggesting that the differential effect is manifest during the recovery form damage and not in response to the initial insult. Whether this effect is responsible for the differences in the chronic response of fibrosis remains to be investigated. However, other groups have reported that crypt cell proliferation and long-term fibrosis may be intricately linked in the intestine.[20,21] In the clinic, after focal radiation therapy the intestinal radiation-induced intestinal injury (including PRT) is a common side effect in patients with gastrointestinal tumors. In cooperative group trials using modest dose (40-50.4 Gy) chemoradiation after resection of pancreatic cancer, severe toxicities (grade 3 or higher) occurred in ~50% of patients.[22] This high rate of severe toxicity has historically limited the radiation dose in abdominal radiation therapy to a lower dose that, not surprisingly, has limited the efficacy or utility of these regimens. In the postoperative setting for pancreatic cancer, local failure rates often exceed 50%.[23] Therefore, the potential of translating our findings to clinical practice could have a significant impact in the management of solid gastrointestinal malignancies using PRT.

Phenomenological or observational studies of classical radiobiological parameters, such as total dose delivered, fractionation, and partial volume irradiation effects using both tumor and normal tissue models, will be critical to understanding clinical FLASH PRT. The available beam parameters (field size, proton range, and modulation) for these studies are currently restricted by the FLASH dose rate requirement, but the operational limits of the proton system have not yet been reached. Finally, clinical trials using veterinary patients will likely prove an invaluable tool that can provide potential clinical benefit to these animals while continuing to develop the extensive technical, biological, and clinical knowledge that will provide the critical underpinnings for clinical trials designed to evaluate FLASH-PRT in humans.

Conclusions

Although it might be too early to discuss clinical translation of FLASH, a few general observations can be discussed. For cyclotron-based double-scatter proton systems, the key limitation will be the maximum field size that can be achieved at a high instantaneous dose rate. The larger the field size, the higher the demand for proton flux will be required at the nozzle. For example, it would require approximately 600 nA of protons at the nozzle to treat a 5 cm x 5 cm field size at 100 Gy/s using the highly efficient plateau region of the high energy beam. This can be challenging because there may be particle loss in the beam transportation system from the accelerator to the treatment room. Pencil beam scanning can theoretically expand the treatment field size by providing high local dose rate to the point of pencil beam, although it may not achieve the overall FLASH dose rate for the entire treatment field. The spot scanning speed can be on the order of 2 to 5 ms for a 5-mm spot-to-spot distance, which provides enough high local dose rate to reach the FLASH condition. The effect of pencil beam scanning is still unknown in animal studies, which will be our future goal as well. The use of Bragg peak region will have further clinical challenges. First reducing effective beam energy to treat shallow targets will result in significant beamline

particle loss owing to the beam optic design and scatter or attenuation of the proton beam through the beam energy degrading process. Although the ionization will be enhanced owing to the slowing-down protons in the Bragg peak region, the ionization may not be sufficient to compensate for the loss of low energy proton flux in the degrading system. It is still unknown if the high linear energy transfer in the Bragg peak would enhance the FLASH effect. However, the high linear energy transfer effect is quite narrow in the depth direction. It is not expected to have a significant impact for large tumor targets while the effect could be significant for smaller targets.

Acknowledgments

Institutional funds were provided by the Department of Radiation Oncology, University of Pennsylvania.

References

1. Favaudon V, Caplier L, Monceau V, et al. Ultrahigh dose-rate FLASH irradiation increases the differential response between normal and tumor tissue in mice. Sci Transl Med 2014;6:245ra93.
2. Durante M, Brauer-Krisch E, Hill M. Faster and safer? FLASH ultra-high dose rate in radiotherapy. Br J Radiol 2018;91:20170628. [PubMed: 29172684]
3. Harrington KJ. Ultrahigh dose-rate radiotherapy: Next steps for FLASH-RT. Clin Cancer Res 2019;25:3–5. [PubMed: 30093447]
4. Vozenin MC, De Fornel P, Petersson K, et al. The advantage of FLASH radiotherapy confirmed in mini-pig and cat-cancer patients. Clin Cancer Res 2019;25:35–42. [PubMed: 29875213]
5. Schmid TE, Dollinger G, Hauptner A, et al. No evidence for a different rbe between pulsed and continuous 20 mev protons. Radiat Res 2009;172:567–574. [PubMed: 19883224]
6. Schmid TE, Dollinger G, Hable V, et al. Relative biological effectiveness of pulsed and continuous 20 MeV protons for micronucleus induction in 3D human reconstructed skin tissue. Radiother Oncol 2010;95:66–72. [PubMed: 20347168]
7. Auer S, Hable V, Greubel C, et al. Survival of tumor cells after proton irradiation with ultra-high dose rates. Radiat Oncol 2011;6:139. [PubMed: 22008289]
8. Buonanno M, Grilj V, Brenner DJ. Biological effects in normal cells exposed to FLASH dose rate protons. Radiother Oncol 2019;139: 51–55. [PubMed: 30850209]
9. Loo BW, Schuler E, Lartey FM, et al. (P003) Delivery of ultra-rapid FLASH radiation therapy and demonstration of normal tissue sparing after abdominal irradiation of mice. Int J Radiat Oncol Biol Phys 2017;98:E16.
10. Montay-Gruel P, Petersson K, Jaccard M, et al. Irradiation in a FLASH: Unique sparing of memory in mice after whole brain irradiation with dose rates above 100 Gy/s. Radiother Oncol 2017;124: 365–369. [PubMed: 28545957]
11. Schuler E, Trovati S, King G, et al. Experimental platform for ultra-high dose rate FLASH irradiation of small animals using a clinical linear accelerator. Int J Radiat Oncol Biol Phys 2017;97:195–203. [PubMed: 27816362]
12. Montay-Gruel P, Acharya MM, Petersson K, et al. Long-term neurocognitive benefits of FLASH radiotherapy driven by reduced reactive oxygen species. Proc Natl Acad Sci U S A 2019;116:10943–10951. [PubMed: 31097580]
13. Spitz DR, Buettner GR, Petronek MS, et al. An integrated physicochemical approach for explaining the differential impact of FLASH versus conventional dose rate irradiation on cancer and normal tissue responses. Radiother Oncol 2019;139:23–27. [PubMed: 31010709]
14. Zlobinskaya O, Siebenwirth C, Greubel C, et al. The effects of ultra-high dose rate proton irradiation on growth delay in the treatment of human tumor xenografts in nude mice. Radiat Res 2014;181:177–183. [PubMed: 24524347]

15. Kim MM, Irmen P, Shoniyozov K, et al. Design and commissioning of an image-guided small animal radiation platform and quality assurance protocol for integrated proton and x-ray radiobiology research. Phys Med Biol 2019;64:135013. [PubMed: 31075786]
16. P A, T BD, K H, et al. Absorbed dose determination in external beam radiotherapy: An international code of practice for dosimetry based on standards of absorbed dose to water. IAEA Technical Report Series 2006;12.
17. Cascio EW, Gottschalk B. A simplified vacuumless faraday cup for the experimental beamline at the Francis H. Burr proton therapy center. 2009 IEEE Radiation Effects Data Workshop 2009;161–165.
18. Verginadis II, Kanade R, Bell B, et al. A novel mouse model to study image-guided, radiation-induced intestinal injury and preclinical screening of radioprotectors. Cancer Res 2017;77:908–917. [PubMed: 28011621]
19. Patriarca A, Fouillade C, Auger M, et al. Experimental set-up for FLASH proton irradiation of small animals using a clinical system. Int J Radiat Oncol Biol Phys 2018;102:619–626. [PubMed: 30017793]
20. Zheng H, Wang J, Koteliansky VE, et al. Recombinant soluble transforming growth factor beta type II receptor ameliorates radiation enteropathy in mice. Gastroenterology 2000;119:1286–1296. [PubMed: 11054386]
21. Skwarchuk MW, Travis EL. Volume effects and epithelial regeneration in irradiated mouse colorectum. Radiat Res 1998;149:1–10. [PubMed: 9421148]
22. Elhammali A, Patel M, Weinberg B, et al. Late gastrointestinal tissue effects after hypofractionated radiation therapy of the pancreas. Radiat Oncol 2015;10:186. [PubMed: 26337917]
23. Murphy JD, Christman-Skieller C, Kim J, et al. A dosimetric model of duodenal toxicity after stereotactic body radiotherapy for pancreatic cancer. Int J Radiat Oncol Biol Phys 2010;78:1420–1426. [PubMed: 20399033]

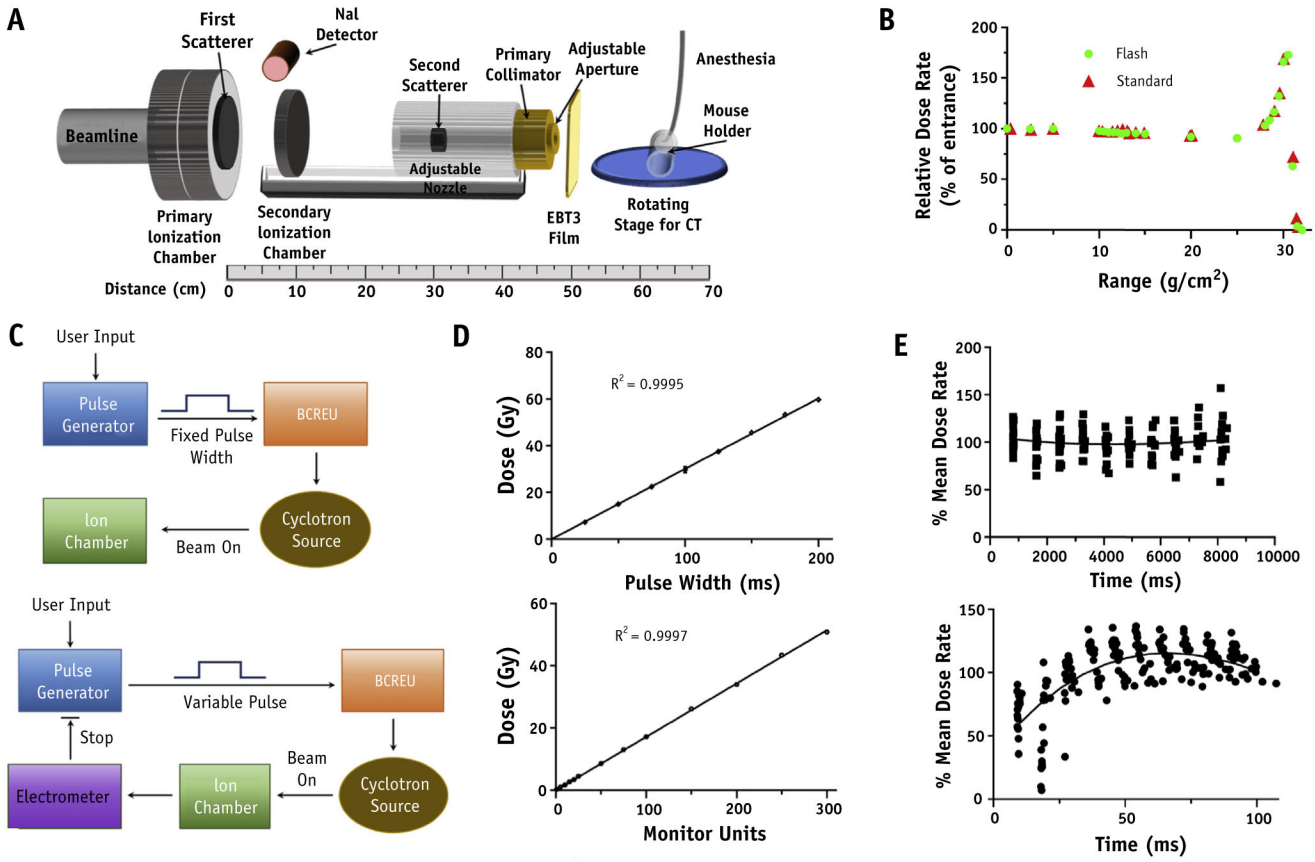

Fig. 1.

Proton radiation therapy set up. Schematic diagram of FLASH proton radiation therapy set up (A). Beam line vacuum ends at the primary ionization chamber (IC) with dual channel readout electrometers interlocked to the primary dose counter and the cyclotron rf chain for a positive failsafe shutoff. After the primary IC is a 2 mm lead first scatterer and secondary IC providing online dose verification. Adjacent to the primary IC exit window, a NaI-gamma detector was introduced for time structure measurements of proton flux. Downstream from the secondary IC is the secondary scatterer consisting of a 5 mm diameter lead shot embedded in a plastic torus which itself is inserted into an acrylic column providing adjustment of distance between scattering centers for optimal beam profile parameters. Custom brass collimators of proton stopping thickness can be inserted into the acrylic column for variation of beam size. (B) Comparison of proton depth dose distribution using FLASH versus standard dose rate. (C) Schematics of proton flux modulation by fixed versus variable pules sent to the beam current regulation unit of the IBA system and (D) linearity of dose versus pulse width or monitor unit count for these designs. (E) Representative dose rate time structure delivered throughout each pulse for standard (18 beam pulses, upper panel) and FLASH (20 beam pulses, lower panel) dose rates.

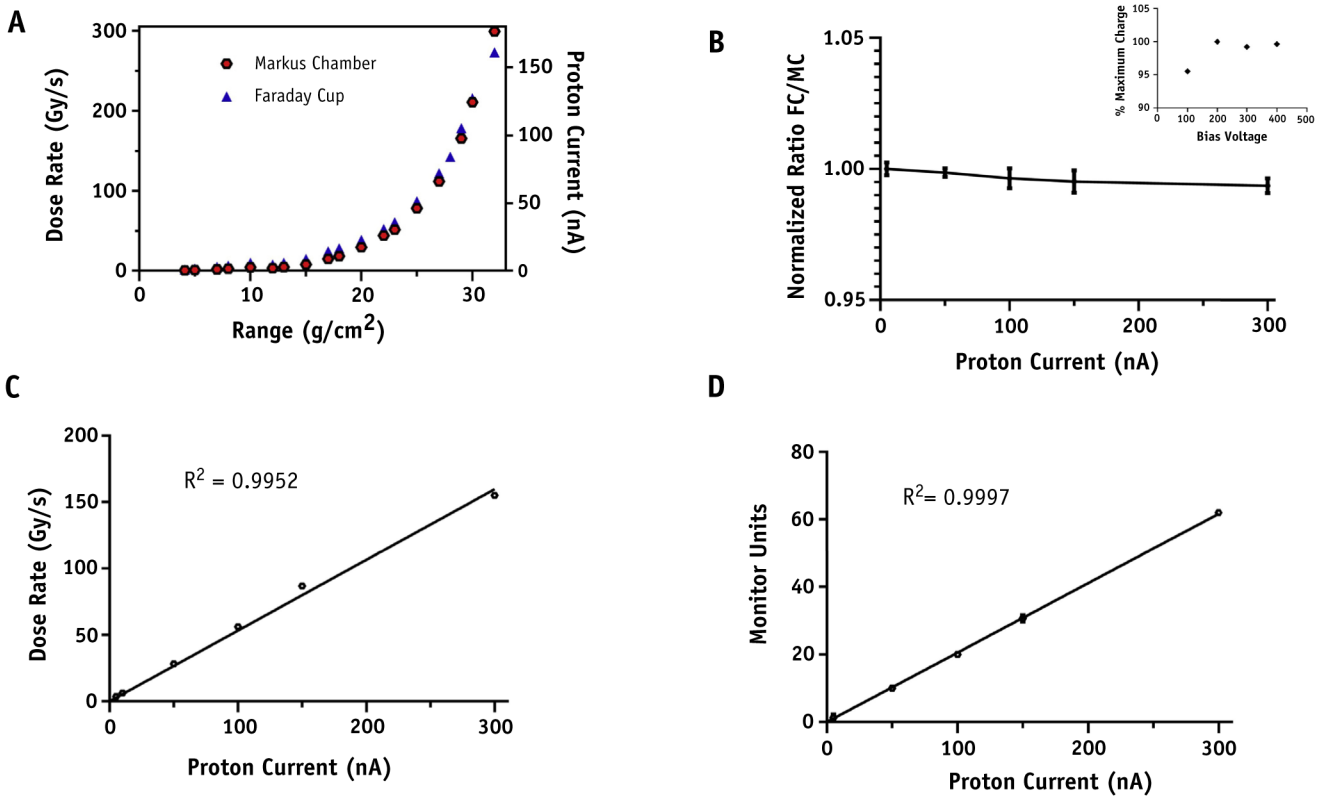

Fig. 2.

Parameters and dose rate verification of FLASH proton radiation therapy set up. (A) Comparison of dose rate measured by Markus Chamber and Proton current measured by Faraday cup versus proton range at target isocenter. (B) Normalized ratio of Faraday cup to Marcus Chamber (MC) readings for proton currents up to 300 nA at a range of 32 g/cm^2 which was used for animal irradiations. MC saturation curve (inset). (C) Dose rate measured using an MC. (D) The secondary ionization chamber MU versus proton beam current for a fixed pulse width of 100 ms.

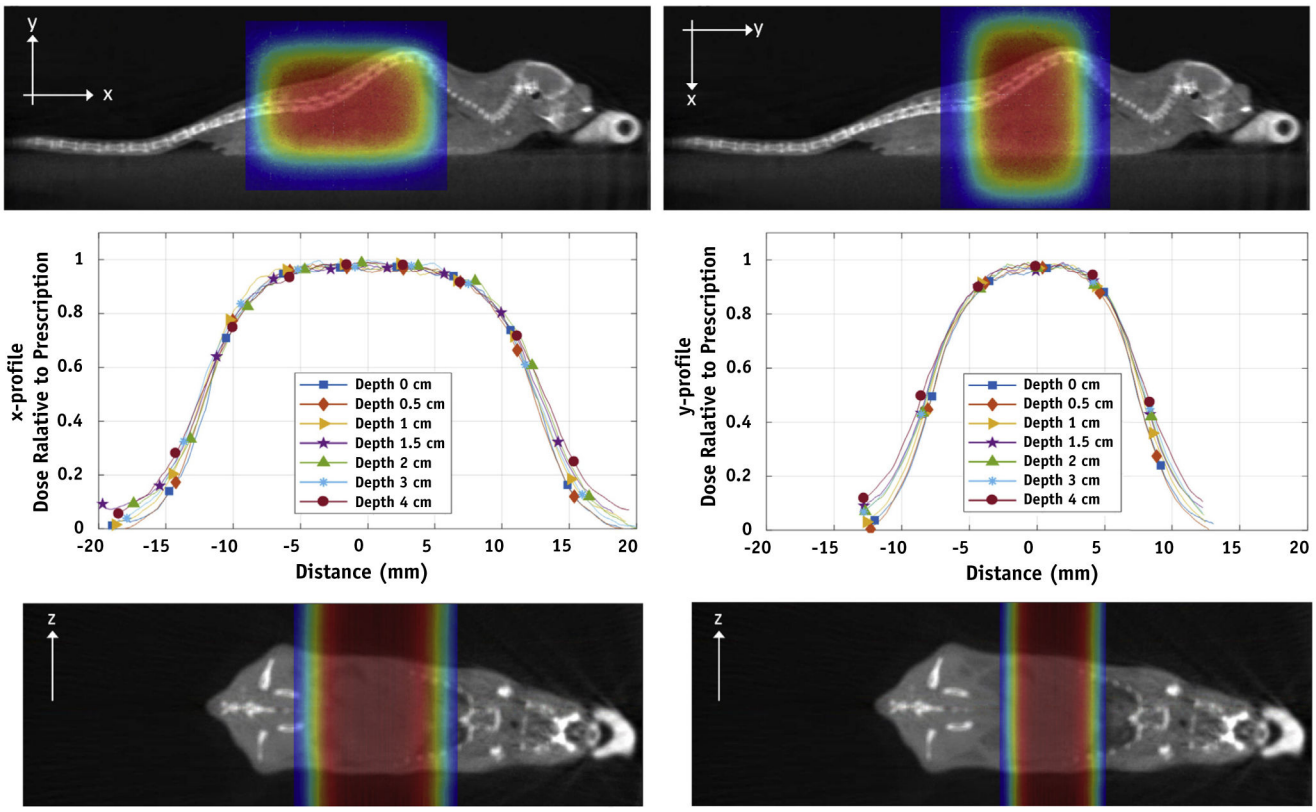

Fig. 3.

Dose distribution for murine experiments. Dose distribution versus depth in solid water was measured with EBT3 film using the double scattered total body set up depicted in Figure 1 for a 1 x 2 cm collimator in either 0- or 90-degree orientation to allow irradiation of whole versus upper abdomen of mice. These data are presented as x-y line profiles (middle panels) and dose color wash using computed tomography aligned beam geometries (upper and lower panels). (A color version of this figure is available at https://doi.org/10.1016/j.ijrobp.2019.10.049.)

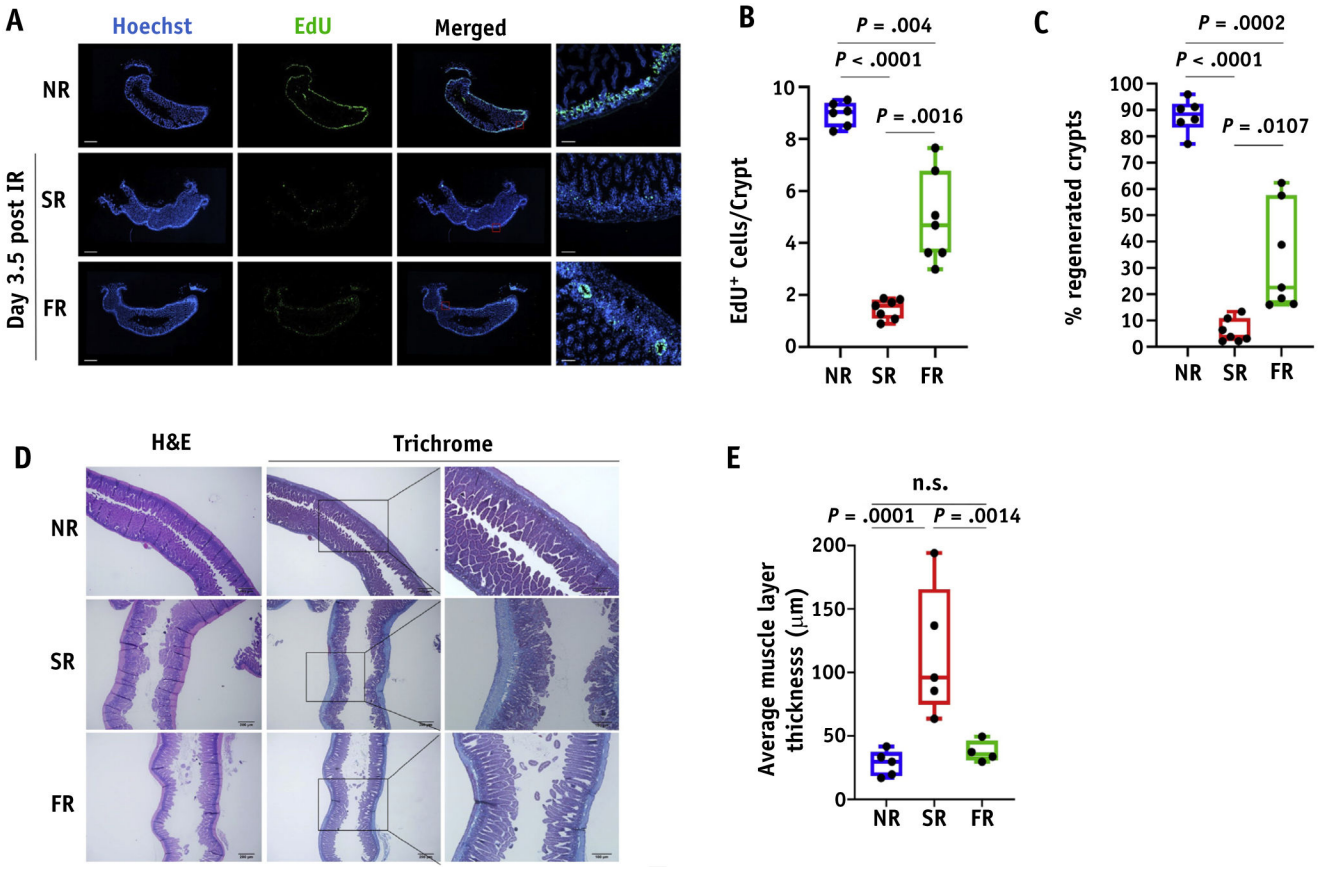

Fig. 4.

FLASH dose radiation preserves better the proliferation of intestinal crypts and inhibits fibrosis formation as a long-term effect post-IR. (A) Representative images of EdU staining in optimal cutting temperature-frozen jejunum sections at 3.5 days post 15 Gy of whole abdominal irradiation (scan of whole tissue, scale bar 1 mm; 10x, scale bar 100 μm). (B) Quantification of EdU + cells per crypt. (C) Quantification of the % regenerated crypts. Data expressed as mean ± SEM. (D) Representative Masson's trichrome stain images of formalin fixed jejunum sections irradiated with 18 Gy at 8 weeks post-IR. (E) Quantification of fibrosis formation by calculating the average muscle layer thickness. Data expressed as mean ± standard error of the mean. *Abbreviation:* n.s. = not significant.

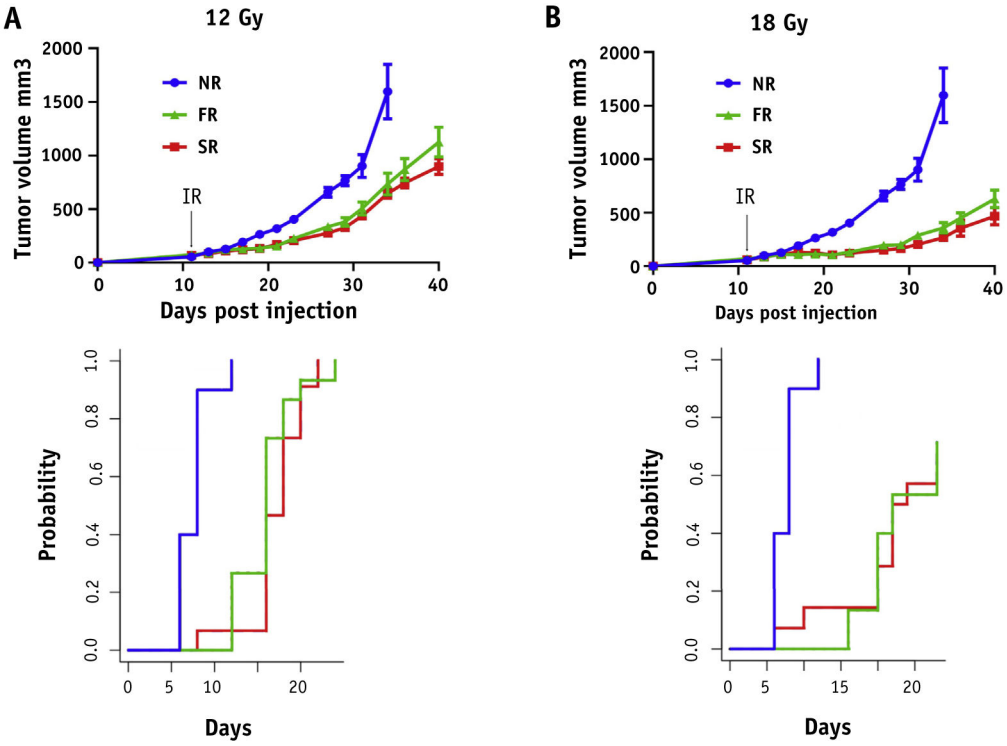

Fig. 5.

FLASH dose rate has no additional impact on tumor growth control. Mice injected with MH641905 cells on their flanks and received 12 (A) or 18 Gy (B) focal irradiation (including tumor and upper intestine) with protons at standard (SR, red) versus FLASH (FR, green) dose rates and followed for tumor growth. Unirradiated mice were served as a control group (NR, blue). Black arrow indicates the time of irradiation. Data expressed as mean ± SEM. Cumulative incidence of tumor regrowth to 4x the starting tumor volume was calculated for each dose (bottom panel) and demonstrated that tumor regrowth was decreased by proton radiation therapy ($P < .000001$), but not different between FLASH and standard proton radiation therapy (12 Gy $P = .68$; 18 Gy $P = .84$). (A color version of this figure is available at https://doi.org/10.1016/j.ijrobp.2019.10.049.)

Table 1

Parameters for experiments in Figures 4 and 5

Experiment	Mouse sex	Age at IR (weeks)	Average weight at IR (g)	Dose (Gy)	Modality	N	Average dose rate (Gy/s)
Whole abdomen	Female	10	19.2	15	FLASH	49	94
					Standard	49	1.0
					Control (0 Gy)	10	N/A
Focal abdomen + tumor	Female	10.5	19.2	12	FLASH	15	63
					Standard	15	0.74
					Control (0 Gy)	5	N/A
				18	FLASH	14	63
					Standard	15	0.71
					Control (0 Gy)	5	N/A

Abbreviations: IR = Irradiation.

Int J Radiat Oncol Biol Phys. Author manuscript; available in PMC 2021 February 01.